Available online at www.sciencedirect.com
ScienceDirect
Microporous and Mesoporous Materials 95 (2006) 329–338
MICROPOROUS AND MESOPOROUS MATERIALS
www.elsevier.com/locate/micromeso

Rare earth exchanged (Ce^{3+}, La^{3+} and RE^{3+}) H–Y zeolites as solid acid catalysts for the synthesis of linear alkyl benzenes

Bejoy Thomas [a,1], Bibhuti B. Das [b], S. Sugunan [a,*]

[a] Department of Applied Chemistry, Cochin University of Science and Technology, Kochi 680 022, India
[b] Department of Physics, Indian Institute of Science, Bangalore 560 012, India

Received 26 November 2005; received in revised form 6 May 2006; accepted 28 May 2006
Available online 20 July 2006

Abstract

Rare earth exchanged H–Y zeolites were prepared by simple ion exchange methods at 353 K and have been characterized using different physicochemical techniques. A strong peak around 58 ppm in the $^{27}Al\{^{1}H\}$ MAS NMR spectra of these zeolites suggests a tetrahedral coordination for the framework aluminium. Small peak at or near 0 ppm is due to hexa-coordinated extra-framework aluminium and a shoulder peak near 30 ppm is a penta-coordinated aluminium species; $[Al(OH)_4]^-$. The vapor-phase benzene alkylation with 1-decene and 1-dodecene was investigated with these catalytic systems. Under the reaction conditions of 448 K, benzene/olefin molar ratio of 20 and time on stream 3 h, the most efficient catalyst was CeH–Y which showed more than 70% of olefin conversion with 48.5% 2-phenyldecane and 46.8%, 2-phenyldodecane selectivities with 1-decene and 1-dodecene respectively.

Keywords: Benzene alkylation; Linear alkyl benzenes; Magic angle-spinning NMR; Rare earth exchanged H–Y zeolites; Solid acid catalysts

1. Introduction

The alkylation of aromatic hydrocarbons is an industrially important synthetic transformation and is applied on a large scale in the chemical industry. Alkylation of benzene with C_{10}–C_{14} linear alkenes is used for the synthesis of linear alkyl benzenes (LABs), which are the primary raw material for the production of LAB sulphonates, a surfactant detergent intermediate [1]. The preferred alkylating agents are alkenes due to their low cost and ease of availability. An important issue in these environmentally conscious days is the choice of the catalysts [2]. Traditionally, the reaction is catalyzed by soluble or liquid Brönsted acids such as H_2SO_4 and HF or Lewis acids like $AlCl_3$ and BF_3, which are highly toxic, generate substantial amount of waste and cause severe corrosion problem (Scheme 1).

Various catalysts were tested for their efficiency to catalyze the reaction. At present, considerable effort are being made to find efficient, stable, reusable, and most importantly environmentally benign solid acid catalysts that can successfully catalyze above reaction [3,4]. The introduction of solid acid catalysts such as zeolites remove the need for quench step, facilitating catalyst reuse through continuous reactions or by the separation of solid phase on work-up. Solid acids are generally much easier and safer to handle [2]. Acidic clays [5–7], heteropoly acids [8–10], metal oxides and sulphates [11,12], immobilized ionic liquids [13], zirconia supported 2-tungstophosphoric acid [14], methanesulfonic acid [15], mesoporous materials [16,17], cation exchange resins [18,19], and various microporous alumino-silicates called zeolites [20–28] have shown good catalytic results (in terms of olefin conversion, LAB linearity and catalyst life time) for the benzene alkylation. A recent paper deals with the use of zeolites H-MOR and MCM-22 for LAB synthesis showing high regioselectivity to 2 and 3-phenyldodecane [29].

* Corresponding author. Tel.: +91 484 2575804; fax: +91 484 2577595.
E-mail addresses: bjoy@sif.iisc.ernet.in (B. Thomas), ssg@cusat.ac.in (S. Sugunan).
[1] Present address: NMR Research Center, Indian Institute of Science, Bangalore 560 012, India. Tel.: +91 80 22932920.

1387-1811/$ - see front matter © 2006 Elsevier Inc. All rights reserved.
doi:10.1016/j.micromeso.2006.05.035

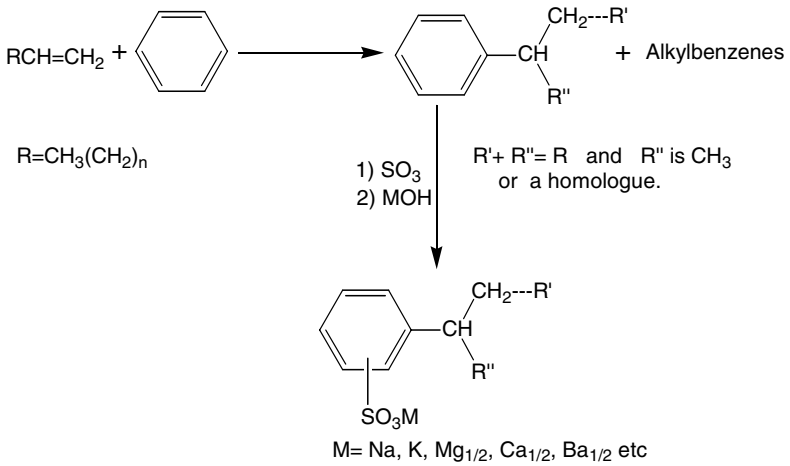

Scheme 1. General scheme showing the alkylation of benzene with higher 1-olefins and subsequent sulfonation leading to the formation of detergents.

The DETAL™ process developed by UOP for the synthesis of LABs is one example of how a more environmentally benign process, which uses solid acid catalyst, can replace the existing conventional technology. This uses solid acid catalysts such as HF supported on amorphous alumino-silicate or silica layers as catalysts in liquid phase reactions [30,31]. The process today is successfully applied in three LAB plants [32].

In the past years rare earth exchanged zeolites have attracted much attention as a stable solid acid catalyst because of their high thermal stability [33]. Modification of zeolites by ion exchange of exchangeable cations provides a useful means of tailoring their properties to particular application. Thus, introduction of rare earth element, in particular into zeolite Y has been an important means of enhancing the performance of, for example, FCC catalyst, and they are known to increase the activity of zeolites in a variety of reactions due to increased acid strength. For example, LaNa–Y plays an important role in the preparation of catalysts for FCC, one of the most widely applied petroleum refining processes that make use of zeolite as catalyst [34].

In this paper, we present the preparation of various rare earth exchanged H–Y zeolites, their physical properties and applicability as catalysts for the vapor-phase alkylation of benzene with higher olefins such as 1-decene and 1-dodecene. Their activities have been compared with standard alkylation catalysts like mordenite zeolite, K-10 clay and silica–alumina. Multinuclear solid state NMR, infrared spectroscopy, energy dispersive X-ray analysis, temperature programmed desorption of ammonia and BET surface area and pore volume measurements were used to characterize H–Y, CeH–Y, LaH–Y and REH–Y zeolites.

2. Experimental section

2.1. Materials and catalyst preparation

Parent H–Y zeolite (Si/Al ratio 1.5) was supplied by Sud-Chemie (India) Ltd. Rare earth zeolites were obtained by contacting H–Y zeolite with a 0.5 M nitrate solution (0.025 mol of nitrate/g of zeolite, obtained from Indian Rare Earths Ltd. Udyogamandal, Kerala) at 353 K for 24 h. All the samples were calcined after exchange at temperatures from 423 to 773 K, and at 773 K for 5 h with a heating rate of 12 K/min with a constant flow of air (60 mL/min). H-mordenite was supplied by Zeolyst International, USA (Si/Al ratio = 19, BET surface area 552 $m^2 g^{-1}$, pore volume 0.266 $cm^3 g^{-1}$ and average crystallite size 0.92 μm). K-10 montmorillonite clay (Si/Al ratio 2.7) was procured from Aldrich Chemical Company, USA. Silica–alumina was prepared by known chemical methods in our laboratory [35]. 1-Decene and 1-dodecene were purchased from Aldrich Chemical Company, USA was used as received. Benzene purchased from SD-Fine Chemicals, India was used after washing with sulfuric acid and 20% Na_2CO_3.

2.2. Catalysts characterization

The chemical composition of rare earth exchanged zeolites was determined by Energy Dispersive X-ray analysis using a JEOL JSM-840A (Oxford make model l6211 with a resolution of 1.3 eV). The crystalline nature of the materials was established by X-ray diffraction studies performed using a Rigaku D-max C X-ray diffractometer with Ni-filtered Cu Kα radiation in an angular range of 2θ from 5° to 50°. Infrared spectra were recorded on a Nicolet Impact 400 FT IR spectrometer.

One-pulse ^{29}Si and proton decoupled ^{27}Al MAS NMR studies were carried out in the magic angle-spinning mode using a Bruker DSX-300 spectrometer at resonance frequencies of 59.63 MHz and 78.19 MHz respectively. For all the experiment a standard 4 mm double-bearing Bruker MAS probe was used. ^{29}Si MAS NMR spectra were recorded with a 4 mm MAS rotor system after a $\pi/2$ single-pulse excitation of 10 μs with repetition time of 5 s. Experiments were performed with a sample rotation frequency of 7 kHz. ^{29}Si chemical shifts were referenced to tetramethylsilane with use of Q_8M_8 as a secondary reference

and setting the highest field peak to −109.7 ppm. An average of 2000 scans was collected for each sample. ^{1}H decoupled ^{27}Al MAS NMR measurements were carried out with 4 mm MAS rotor system. Pulse length of the aluminium $\pi/2$ pulse was 4 μs and repetition time for the experiments was 5 s. All spectra were collected at a spinning rate of 8 kHz. ^{1}H decoupling applied during the acquisition time was found to have noticeable effect on the width of the peaks in the ^{27}Al spectrum. Chemical shifts were represented with reference to $Al(NO_3)_3$ peak at 0 ppm. The average number of scans collected for the experiments were about 2000–3000 for the samples.

Acid structural properties were estimated using temperature programmed desorption (TPD) of ammonia with conventional equipment. BET surface area measurements were performed using a Micromeritics Gemini surface area instrument using di-nitrogen as an adsorbate at 77 K. The area per molecule of di-nitrogen was taken as 16.2 $Å^2$. This protocol gave specific surface area and also the total pore volume of the materials.

2.3. Catalytic reaction

Catalytic reactions were carried out in an ordinary fixed-bed, down-flow reactor made of cylindrical quartz tube with 0.6 cm internal diameter and 30 cm height with a high sensitivity temperature controller (accuracy ±5 K) and a set up to carryout reaction under gaseous atmosphere. The catalysts particles (1500 mg and 30–40 μm mesh size) were filled between ceramic beads. During the operation, the gaseous reactants flow through the reactor tube and over the catalysts bed, and reaction takes place. Nitrogen was used as carrier gas in the reaction. Prior to alkylation reaction, catalysts were heated *in situ* at a heating rate of 20 K/min to a final temperature of 773 K in presence of constant purging of air and was maintained at the final temperature for 12 h. The catalyst was then allowed to cool to reaction temperature (448 K) under dry nitrogen flow (10 mL/min) and kept for 1 h before the commencement of reaction. Benzene and olefin in appropriate molar ratio was fed into the reactor at flow rate of 4 mL/h (WHSV = 2.46 and 2.45 h^{-1} or contact time = 0.407 and 0.408 h respectively for two alkenes) by means of an infusion pump. The rate of product withdrawal was brought into equilibrium with introduction of the reactant by controlling the pilot valve at the bottom of the reactor. Products on the stream were periodically collected and analyzed using a Chemito GC1000 Gas Chromatograph fitted with an FID detector and SE-30 capillary column. Column temperature was adjusted between 383 K and 548 K, injector temperature was 523 K and detector temperature was 523 K. Isomer identification was done using a Shimadzu QP 2010-GCMS with 30 m universal capillary column of cross-linked 5% phenylmethylsilicone. The MS detector voltage was 1 kV. The m/z values and relative percentage intensity are indicated for the significant peaks. (Column temperature; 323–533 K and heating rate was 10 K/min, injector; 513 K and detector; 563 K.) The conversion of olefin and selectivity for the 2-phenylalkane was calculated according to the method proposed by de Almeida et al. [36].

3. Results and discussion

3.1. Physicochemical characteristics

Chemical composition of the parent and different rare earth exchanged zeolites are seen in Table 1. Results were reproducible within an error limit of 4%. X-ray diffraction and infrared spectral studies confirm that the zeolite framework remains intact even after ion exchange at moderately high temperatures. Consistent with the earlier reports, the parent as well as rare earth exchanged zeolites crystallizes into cubic unit cell with F3dm space group. Major shift in the framework vibrational band positions in infrared spectroscopy is shown in Table 1. Details of the physical characteristics are reported in our previous communications [37].

Determination of acidic/basic sites on solid surfaces is a multifaceted problem and unfortunately there exists no general theory of the acidity or basicity of the solids that could serve as a basis for their determination. Zeolites are generally categorized as acidic materials although basic sites too exist on these. It will be interesting to analyze, in

Table 1
Chemical composition and framework vibrational band shifts (400–1300 cm^{-1}) as observed by infrared spectral studies on H–Y and different rare earth zeolites

Zeolite	Chemical composition[a]	Asymmetric stretch (cm^{-1}) EL or IT[b]	Symmetric stretch (cm^{-1}) EL or IT[b]	Double ring[c] (cm^{-1})	T–O bend[d] (cm^{-1})
H–Y	$H_{76.5}Al_{76.5}Si_{115.5}O_{384}$	1050	771	570	457
CeH–Y	$Ce_{14.06}H_{34.07}Al_{76.25}Si_{115.57}O_{384}$	1083	790	574	480
LaH–Y	$La_{15.44}H_{29.23}Al_{76.25}Si_{115.75}O_{384}$	1061	771	572	463
REH–Y[e]	$La_{9.01}Ce_{1.68}Pr_{3.91}Nd_{4.28}H_{18.78}Al_{75.42}Si_{116.58}O_{384}$	1072	772	573	469

[a] As determined by energy dispersive X-ray analysis.
[b] EL, external linkage; IT, internal tetrahedra.
[c] D_6R double ring units.
[d] T = Si, Al.
[e] RENa–Y is a mixed rare earth exchanged zeolite with La^{3+} as the main counter cation and small amounts of Ce^{3+}, Pr^{3+} and Nd^{3+}.

Table 2
Textural and acid structural properties of different zeolites, K-10 clay and silica–alumina

Catalyst	Amount of ammonia (mmol/g^{-1}) desorbed within certain temperature range K				Textural properties	
	W[a,b]	M[a]	S[a]	Total	Surface area[c] (m^2/g)	Pore volume[d] (scc/g)
H–Y	0.69	0.41	0.33	1.43	398	0.266
CeH–Y	1.10	0.60	0.31	2.02	511	0.340
LaH–Y	0.51	0.71	0.46	1.68	464	0.288
REH–Y	0.68	0.86	0.49	2.03	483	0.301
K-10-Mont.	0.55	0.24	0.13	0.92	183	0.204
SiO_2–Al_2O_3	0.55	0.18	0.10	0.83	168	0.179

[a] The ammonia desorbed in the temperature range 373–473 K might contain small amounts of physisorbed ammonia also.
[b] W, M, and S stand for weak (373–473 K), medium (474–673 K), and strong (674–873 K) acid sites.
[c] BET surface area.
[d] Total pore volume measured at relative pressure of 0.9976.

this context, the order of acidity among different rare earth zeolites on the basis the nature of the cations. Table 2 describes the distribution of acidity in three temperature regions of 373–473 K (week acid sites), 473–673 K (medium strength acid sites) and 673–873 K (strong acid sites). The data on the chemisorption of ammonia in zeolites at different temperatures as obtained from step-wise thermal desorption is presented in our previous communication [37a]. For H–Y and LaH–Y zeolites the amount of ammonia desorbed decrease gradually as the temperature increase. CeH–Y and REH–Y zeolites show an increase in the amount of ammonia chemisorbed at 673 K. All zeolites invariably show higher desorption at low temperatures probably due to the interaction of ammonia with non-acidic sites and is more in the case of rare earth exchanged zeolites. A similar observation is already been reported in the case of mordenite zeolite [38]. Hence the number of acid sites measured by the ammonia chemisorption at lower temperatures can be taken only as an upper limit of the acid sites in the zeolites. However, at higher temperatures (>623 K) the non-acidic ammonia interactions are weak and hence the sites measured by chemisorption of ammonia are expected to be acidic ones. This part is considerably larger in the case of all the rare earth exchanged zeolites compared to H–Y. This supports the enhancement in acid structural properties upon rare earth exchange.

Surface area and pore volume increase invariably on exchange with rare earth cations (Table 2). The increase of surface area might be due to the decrease in the crystallite size and improvement in the microporous nature on exchange of hydrogen in H–Y zeolite with rare earth cations. K-10 clay is a layered alumino-silicate with a dioctahedral layer sandwiched between two tetrahedral layers. Unlike zeolites used, K-10 clay does not have a regular pore structure [39]. The pore size >1.0 nm is an average value. The structure of the clay is constituted of both micropores and mesopores. The amount of mesopores is less when compared to the amount of micropores. Silica–alumina is a porous solid without regular pores and has lower surface area and pore volume compared to zeolites.

3.2. Aluminium NMR studies

^{1}H decoupled ^{27}Al MAS NMR spectra of H–Y, CeH–Y, LaH–Y, and REH–Y zeolites are shown in Fig. 1. All the zeolites show a strong peak around 58 ppm, and a small peak around 0 ppm corresponding to those of tetrahedral

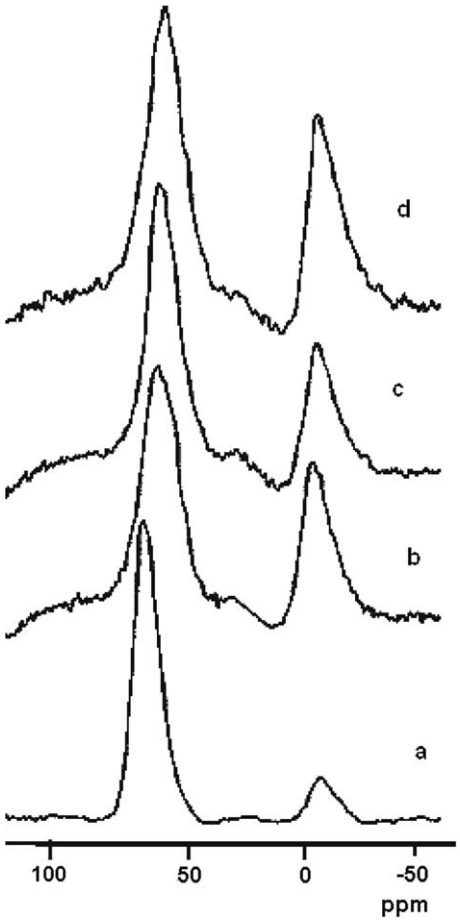

Fig. 1. ^{27}Al {^{1}H} magic angle-spinning NMR on zeolites (a) H–Y, (b) CeH–Y, (c) LaH–Y, and (d) REH–Y recorded with a resonance frequency of 78.19 MHz for ^{27}Al and 300.08 MHz for ^{1}H with a sample spinning speed of 8.0 kHz.

and Al as expected for Y-type zeolite. The intensity of the octahedral peak increases on rare earth exchange. This is rather expected as there is possibility of formation of non-framework aluminium upon thermal exchange and subsequent high temperature activation. The full width half maximum (FWHM) for both the peaks of the H–Y and different rare earth exchanged zeolites have been calculated. There is a small peak at 3.74 ppm for H–Y zeolite and is assigned to octahedral aluminium. The $^{27}Al\{^{1}H\}$ MAS NMR experiments also confirm the presence of penta-coordinated aluminium, $[Al(OH)_4]^-$ (shoulder peak around 30 ppm) in H–Y and rare earth exchanged zeolites. Simple MAS NMR spectra (not shown) have not provided clear information about this aluminium species. The peak positions are 29.81, 31.21, and 30.81 ppm respectively for CeH–Y, LaH–Y, and REH–Y zeolites. The penta-coordinated aluminium peak is more prominent in the case of rare earth exchanged zeolites.

Rare earth exchange not only increases the intensity of the octahedral peak but also shift its position from 3.74 ppm to around 0 ppm. The peak positions are 0.23, −0.54, and −0.47 ppm respectively for CeH–Y, LaH–Y, and REH–Y zeolites. Similarly the peak position for the tetrahedral aluminium also shifted on exchange with rare earth metal ions. The peak positions are 59.85, 55.33, 56.14, and 55.74 ppm for H–Y, CeH–Y, LaH–Y and REH–Y zeolites. The up-field shift in the peak position is correlated to the strain in the T–O–T framework in presence of bulky rare earth metal ions [40–42]. As shown by NMR spectral studies, lanthanum exchanged H–Y zeolite exhibits rather unusual peak position when compared to CeH–Y or REH–Y zeolites. This is explained as an effect of migration of La^{3+} ions from supercage cation locations to small cage positions in the zeolite structure. Increase in the intensity of octahedral peak confirms possibility of dealumination during catalyst preparation. However, these non-framework aluminium centers acts as potential Lewis acid-centers during catalytic reactions.

3.3. Silicon NMR studies

High resolution solid state silicon-29 NMR spectroscopy is a powerful tool for investigating the structure and nature of bonding characteristics in zeolites. It is useful for the determination of Si, Al ordering in tetrahedral aliminosilicate framework, monitoring the structural recognition of TO_4 ($T = Si^{4+}$ or Al^{3+}) unit upon dealumination [40–44], and detecting temperature induced phase transitions in silicalite. The complex compositional dependence of the position and shape of the five Si(*n*Al) bands provides information sufficient to determine local Si, Al order in FAU type zeolites [43b]. The spectrum of pure H–Y zeolite shows five peaks at −83.9, −93.5, −98.7, −105 and −111.6 ppm, which are attributed to Si(4Al0Si), Si(3Al1Si), Si(2Al2Si), Si(1Al3Si) and Si(0Al4Si) tetrahedral silicon units respectively, in which Si(*n*Al) denotes Si atom coordinated by *n*Al atom and $(4 - n)$ silicon atom through oxygen atoms. Rare earth exchanged H–Y zeolites show similar patterned spectra. In general, spectra are broad and different Q-units are not well-separated. However, the whole shape is similar to the spectrum of H–Y. Various Q-units in rare earth zeolites are up-field shifted by 1–2 ppm and the results are shown in Fig. 2. Q^4; Si(0Al4Si) peak of H–Y is shifted from −111.6 ppm to −113.9 in case of CeH–Y and LaH–Y and −113.2 ppm in case of REH–Y zeolite.

Lippmma and co-workers have already demonstrated the regular dependence of the ^{29}Si chemical shifts on the number of alumina tetrahedra linked via oxygen bridges, to each SiO_4^{4-} tetrahedron [45]. As a reason for the high-field shift of the Si(*n*Al) signal on rare earth exchange, a variation of the local structure of AlO_4 tetrahedra in the vicinity of the resonating silicon atoms due to the presence of bulky and heavily charged rare earth cations and an effect of cationic extra-framework aluminium (hexa-coordinated aluminium formed via leaching from the framework) were widely reported [42b,43]. Each rare earth cation satisfies single negative valency of 3 aluminium tetrahedra in the framework and this induce considerable strain in the zeolite framework. Substantial shifts in the framework vibrational band positions as seen in Table 1 is a measure of this strain and is reflected in the Si(*n*Al) signal positions. The repulsive interactions of protons and the rare earth ions enhance the migration of rare earth ions from supercage cation position to small cage cation locations. This kind of cation migration may affect the position of the peak and reduces the number of accessible Brönsted acid sites on

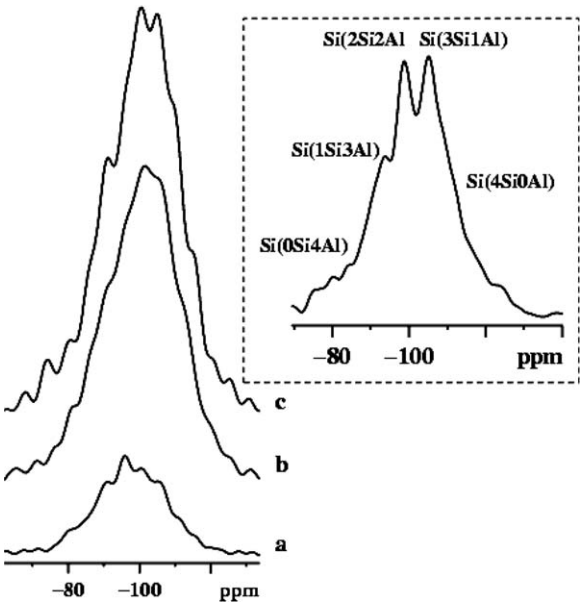

Fig. 2. One-pulse ^{29}Si MAS NMR spectra of zeolites (a) LaH–Y, (b) REH–Y and (c) CeH–Y recorded at a resonance frequency of 59.63 MHz with sample spinning speed of 7 kHz. The spectrum shown in inset is silicon-29 MAS NMR spectra of parent H–Y zeolite recorded under similar conditions and has been assigned based on chemical shifts of different silicon units with respect to standard TMS peak at 0 ppm.

rare earth zeolites [46,47]. This indicates that the ^{29}Si NMR peaks are influenced by the counter cations in the extra-framework cation locations.

3.4. Alkylation reaction

3.4.1. Effect of reaction variables

Vapor-phase reactions were performed under constant flow of nitrogen. The effect of reaction temperature, catalyst loading, and benzene to olefin molar ratio were examined in order to optimize the conversion of olefin and selectivity to the monoalkylated product or more precisely the 2-phenyl isomer formation.

3.4.2. Effect of temperature

Fig. 3A shows the effect of reaction temperature in the vapor-phase alkylation of benzene with 1-dodecene. Reaction temperature was varied between 408 K and 523 K over H–Y zeolite. The conversion of 1-dodecene increases with increase in the reaction temperature (49.1% at 408 K increased to 78.3% at 523 K). However, the increase in conversion is at the cost of selectivity for 2-phenyl isomer. This can be due to the increasing probabilities of catalytic cracking, rapid equilibration of the olefin isomer or easy diffusion of the bulkiest LAB isomers out of the zeolite cavities at higher temperatures. By comparing the results, in general, we can say that temperature has a positive influence on alkylation of benzene with C_{10} and C_{12} olefins.

3.4.3. Influence of catalyst loading

Total conversion of 1-dodecene and selectivity for monoalkylated product as a function of catalyst loading is displayed in Fig. 3B. Reactions were performed by keeping WHSV constant at 2.45 h^{-1}. As the amount of catalyst increases, total conversion of olefin increases. However, at the same time there is slight decrease in the formation of monoalkylated product. Formation of heavy isomers seems to increase with the amount of catalyst. With an increase in the catalyst loading, opportunity for the reaction on external acid sites increased and consequently the conversion of alkene increased. However, at the same time the selectivity for the 2-phenylalkane decreased from 47.5% to 42.2%.

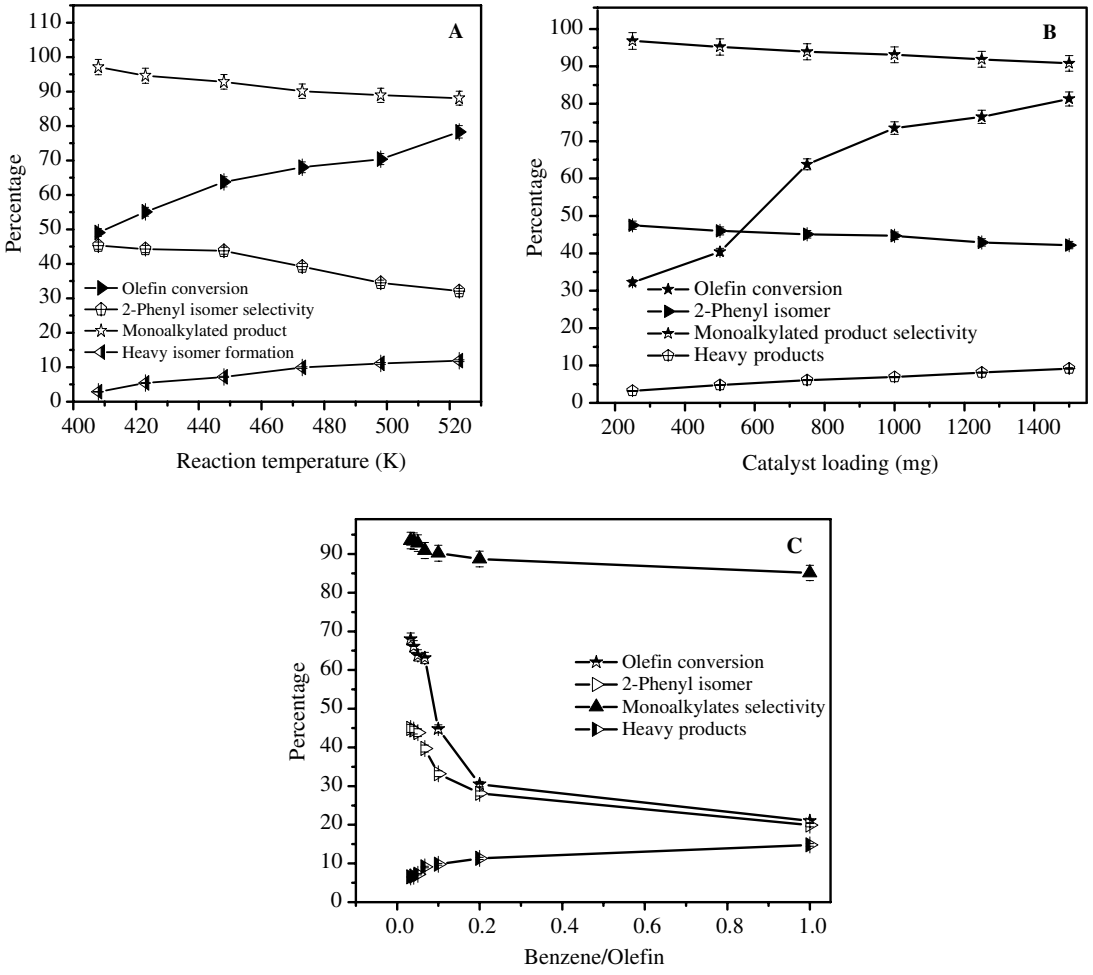

Fig. 3. Influence of reaction variables during the alkylation of benzene with 1-dodecene over H–Y zeolite, (A) effect of reaction temperature, (B) effect of catalyst loading and (C) 1-dodecene to benzene molar ratio. The standard and maximal deviations are marked by error bars.

3.4.4. Effect of olefin to benzene molar ratio

Fig. 3C shows influence of molar ratio of the reactants on the conversion and selectivity of the alkylation reaction. Conversion decreased from 66.1% to 21% on increasing the alkene to benzene molar ratio from 0.033 to 1. However, selectivity for the 2-phenyl isomer is increased from 19.9% to 44.5% on increasing the molar ratio from 1:1 to 1:20. However, the formation of heavy isomers is decreased from 14.9% to 6.4%. As the reversible reaction reaches equilibrium state, an increase in the amount of benzene leads to an increase in the conversion of olefin. Increase in the 2-phenylalkane selectivity could be explained in terms of solvation effect of benzene in higher molar ratios. In the alkylation of benzene with 1-dodecene, the solvation of the reaction intermediates by the solvent molecules apparently reduces the differences in the stabilities of carbocations, which ultimately results in greater formation of 2-phenyldecane.

3.4.5. Performance of different catalytic systems

Table 3 summarizes the experimental results of alkylation of benzene with detergent range olefins; 1-decene and 1-dodecene on H–Y, rare earth exchanged (Ce^{3+}, La^{3+} and RE^{3+}) H–Y and mordenite zeolites, K-10 clay and silica–alumina. In general, 1-dodecene conversion is more compared to 1-decene and is in the expected lines. The effect of alkylating agent on the rate of Friedel–Crafts reaction is well-documented in the literature [48]. Among different Y zeolites, pure H–Y converts maximum olefin. Exchange of H^+ ions with rare earth metals decrease the total olefin conversion considerably. However, this is at the expense of corresponding increase in the selectivity of the 2-phenyl isomer formation. In the rare earth zeolites series, highest conversion of 76.3% and 76.5% for the two olefins is exhibited by CeH–Y zeolite.

There is much difference in the product distribution for both alkenes. This difference in the product distribution is explained as follows. The alkylation of benzene with 1-alkenes goes through a carbocation mechanism. This carbocation undergoing rapid isomerization in varying degrees and finally attacks benzene in what is considered to be the rate determining step to form the product. The intermediate carbocation undergoing a series of fast hydride shifts produces isomeric ions. The hydride transfers, though very rapid, are not instantaneous [49], and therefore, some of the carbocation may react with aromatic ring before undergoing rearrangement [50]. Therefore, isomerization of the carbocation to internal isomers in the carbon chain is not fast enough to allow isomeric ions to attain equilibrium before they attack benzene. In the present case this thermodynamic equilibrium is not probably reached. Greater 2-phenyl isomer content in the product mixture suggests a non-attainment of thermodynamic equilibrium. Under the present reaction conditions the intermediate carbocation from 1-decene and 1-dodecene do not come to equilibrium before they attack the aromatic ring or the rate of alkylation step is not sufficiently low to allow isomerization of the intermediate to proceed to the most stable distribution. The relative stabilities of the carbocations increase towards the center of the carbon chain, the least stable being the primary ion (C_1-position). In fact due to its very low stability, the 1-phenylalkane is not at all detected. On the basis of this, one would expect the isomer content to increase with the carbon number (towards the center of the olefin chain). This is possible only if the thermodynamic equilibrium is reached before the carbonium ion attacks benzene. This is found to be so in the case of HF acid in which thermodynamic equilibrium is probably reached [50].

In all the cases there was formation of small amounts of tertiary alkylbenzene (<2%) indicating the probabilities of skeletal isomerization of the intermediate ions. However, the rate of skeletal isomerization is low compared to the rate of alkylation or hydride shifts due to the mild reaction conditions. Actually, skeletal isomerization of 1-dodecene in presence of acid catalyst has been reported even at 348 K and observation of small amounts of such reaction products in the mixture is not surprising [51].

Table 3
Total conversion and selectivities for different products during the alkylation of benzene with C_{10} and C_{12} olefins over parent H–Y, various rare earth exchanged H–Y, H-MOR zeolites, K-10 clay and silica–alumina

Catalyst	1-Decene (%)				1-Dodecene (%)			
	Conversion	Monoalkylated[a]	Heavy products[b]	2-Phenyl decane	Conversion	Monoalkylated[a]	Heavy products[b]	2-Phenyl dodecane
H–Y	79.5	90.4	9.6	43.3	81.9	92.8	7.2	39.2
CeH–Y	76.3	93.3	6.7	48.5	76.5	94.0	6.0	46.8
LaH–Y	68.7	93.8	6.2	47.8	69.2	94.9	5.1	45.9
REH–Y	68.9	92.3	7.7	46.4	69.2	94.1	5.9	45.4
H-MOR	84.2	93.8	6.2	59.1	86.5	94.1	5.9	54.5
K-10 Clay	38.9	93.1	6.9	38.7	39.1	95.2	4.8	34.0
SiO_2–Al_2O_3	27.4	95.9	4.1	33.1	30.2	95.3	4.7	30.2

Reaction temperature; 448 K, amount catalyst; 1500 mg, benzene to olefin molar ratio; 20:1, time on stream; 3 h, constant flow of nitrogen; 10 mL/min. There will be small amounts of non-volatile products, which could not be detected by GC or GCMS.

[a] Include 3, 4, 5, and 6 phenylalkane isomers (however, for 1-decene up to five isomers).

[b] Include decene and dodecene dimers, dialkylbenzenes, alkyltetralenes and some other polymeric.

We have compared the activity of pure H–Y and different rare earth H–Y zeolites with standard catalytic systems such as H-mordenite zeolite, K-10 montmorillonite clay and silica–alumina. Mordenite is known to have an effective unidirectional pore system and as a consequence shows highest conversion of olefins and selectivity to the desired 2-phenyl isomer. In this case, shape selectivity appears to play an important role producing maximum 2-phenyl isomer [52]. K-10 clay and silica–alumina with their weak acidic strength exhibit low conversion of olefins and selectivity for the desired 2-phenylisomer. Least selectivity for the desired product in the case of silica–alumina could be due to its irregular pore system.

3.4.6. Deactivation, reusability and heterogeneity studies

The catalysts were found to be deactivated after prolonged use [53]. Thermal analysis of the deactivated catalysts shows a significant weight loss at ca. 773 K. This is in addition to a lower temperature weight loss, which can be attributed to the adsorbed product. The higher temperature weight loss is possibly due to alkene oligomers, which will block small pores and accompanying exotherm could be result of the deoligomerization. These results suggest that the loss in catalyst activity is due, in part, to blockage of pores with alkylation products and oligomerized alkenes.

The deactivated zeolites can be partially regenerated by solvent extraction to remove most of the 'heavy' products followed by oxidative treatment at the activation temperature. The deactivated catalyst was taken out from the reactor, extracted continuously with diethyl ether for many times and dried in an air-oven at 383 K overnight. It was then calcined as described in Section 2. Carrying out reaction with the regenerated sample, we could get a maximum conversion of 81.0% with H–Y zeolite after 3 h of reaction was observed, which is very close to the conversion obtained for the fresh catalyst.

Alkylation of benzene with 1-dodecene was carried out for 10 h continuously over H–Y, CeH–Y zeolites and products were collected at intervals of 1 h. The results of the studies are depicted in Fig. 4A and B. Conversion of 1-dodecene attains a maximum after 4 h (82.8%) and then starts to deactivate on H–Y zeolite. However, the selectivity for 2-phenyl isomer increases slowly with time and reaches maximum after 10 h (45.1%). CeH–Y undergoes rather slow deactivation compared to H–Y. Conversion was 76.5% at 4 h and 59.2% at the end of the reaction and the corresponding selectivity for 2-phenyalkane was 46.9% and 50.9% respectively. H–Y zeolite underwent 37.1% deactivation whereas, CeH–Y 22.6% in 10 h. The improvement in the 2-phenyldodecane content with time is clearly due to the blocking of unwanted pores of the catalyst upon coking. It practically prevents the diffusion of isomerized products like 3, 4, 5 or 6-phenyldodecane coming out of the zeolite pores. This could also be due to transalkylation reaction between benzene and bidodecylbenzene and tridodecylbenzene in the zeolite pore mouth as established by Da and co-workers [53c]. The increase in the 2-phenyl isomer production is strongly supported by a corresponding decrease in the dialkylate formation with time (Fig. 4A and B).

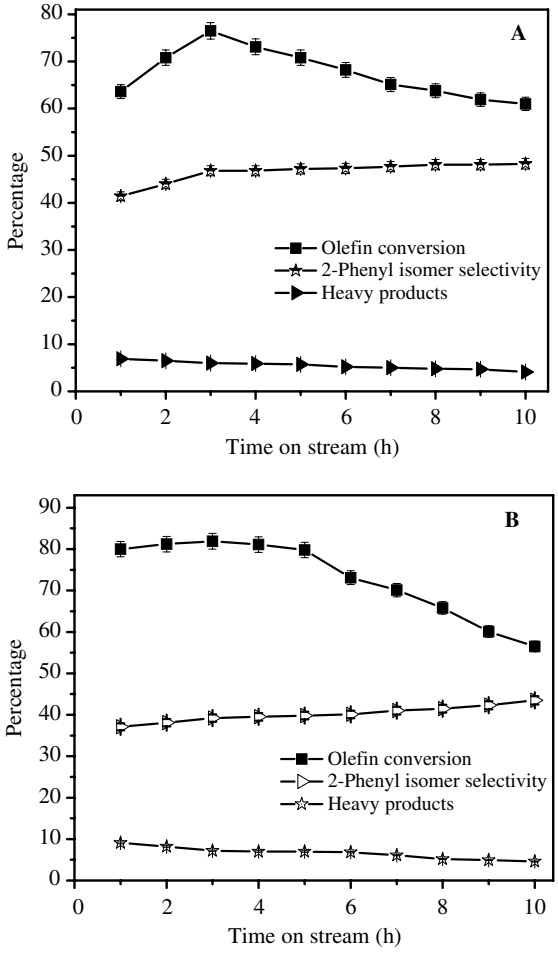

Fig. 4. Influence of time on stream on the alkylation of benzene with 1-dodecene on CeH–Y (A) and H–Y (B) zeolites. Reaction conditions are as described in Table 3. The standard and maximal deviations are marked by error bars.

We have conducted experiments to obtain clear evidence for the true heterogeneity of the reaction. The reaction mixture was passed through H–Y and HCe–Y zeolites under standard reaction conditions for 10 h. No aluminium was detected in the reaction mixture by the energy dispersive X-ray analysis. Furthermore, no Al was detected while qualitative analysis of the mixture also. These results strongly suggest against the possible aluminium leaching during the reaction.

4. Conclusions

Rare earth exchanged H–Y zeolites were prepared by simple ion exchange methods and characterized by different physicochemical techniques. ^{1}H decoupled ^{27}Al MAS NMR spectra of all zeolites show a strong band around 58 ppm confirming the tetra coordination of aluminium

in the structure. The spectra also show small shoulder peaks around 30 and 0 ppm corresponding to penta and hexa-coordinated aluminiums respectively. In the one-pulse ^{29}Si MAS NMR spectra central single peak corresponds to Q^2 Si(2Al) unit. Shoulder peaks represent other silicate units – Q^4, Q^3, Q^1 and Q^0. Size and charge of the counter cation has marked influence on the ^{29}Si MAS NMR chemical shift positions. Friedel–Crafts alkylation of benzene with higher olefins such as 1-decene and 1-dodecene were carried out over these catalysts and their activities have been compared with some common alkylation catalysts such as K-10 clay, H-MOR zeolite and silica–alumina. Taken together, the present studies clearly show that the rare earth exchanged zeolites could be efficient catalysts in the intermolecular coupling of the aromatic nucleus with activated compounds like long chain olefins under relatively mild reaction conditions in a continuous down-flow type reactor. Both the model reactions resulted in excellent yields of coupled products; mainly the 2-phenylalkane. HCe–Y is the best catalyst in the Y zeolites series. Conversion of olefin and selectivity for 2-phenylalkane over HCe–Y zeolite was 76.3% & 48.5% and 76.5 & 46.8 respectively with 1-decene and 1-dodecene. However, these catalysts are susceptible for deactivation caused mainly by the squeezing of bulkier molecules, namely monoalkylbenzene, bialkylbenzene, and trialkylbenzene inside the pores of the catalysts. These are too bulky to diffuse quickly from the intracrystalline pores of zeolites, so they deposit first in these intracrystalline pores and then gradually in the larger pores. Rare earth exchanged zeolites exhibit far better stability towards reaction conditions and on an average they lost almost 20% of their initial activity in 10 h on stream whereas, H–Y lost 37.1% activity with same time on stream. Mordenite underwent maximum deactivation during the reaction and lost nearly 40% of its initial activity.

Acknowledgments

We are thankful to Dr. Sreedharan Prathapan, Reader, Department of Applied Chemistry, Cochin University of Science and Technology and Dr. G.R. Vasanthakumar, Molecular Biophysics Unit, Indian Institute of Science Bangalore for helpful discussion. Funding for this work was provided by the State Council of Science, Technology and Environment, Govt. of Kerala, India. B. Thomas is thankful to CSIR, Govt. of India for Senior Research Fellowship.

References

[1] J.A. Kocal, B.V. Vora, Appl. Catal. A: Gen. 221 (2001) 295.
[2] (a) J.H. Clark, Green Chem. 1 (1999) 1;
(b) J.H. Clark, Pure Appl. Chem. 73 (2001) 103;
(c) R.A. Sheldon, Pure Appl. Chem. 72 (2000) 1233;
(d) J.D. Sherman, Proc. Natl. Acad. Sci., USA 96 (1999) 3471.
[3] A. Corma, Chem. Rev. 95 (1995) 559.
[4] A. Corma, H. Garria, Chem. Rev. 103 (2003) 4307.
[5] H.M. Yuan, L. Zhonghui, M. Enze, Catal. Today 2 (1988) 321.
[6] L. Zhonghui, S. Guida, in: B. Drazoj, S. Hoecevar, S. Pejovnik (Eds.), Zeolites, Stud. Surf. Sci. Catal., vol. 24, Elsevier, Amsterdam, 1985, p. 493.
[7] J.L. Berner Tejero, A.M. Danvila, US Patent, 5, 146, 026, 1992 to petroquimica Espanola S.A. (PETRESA) Spain.
[8] C. Hu, Y. Zhang, L. Xu, G. Peng, Appl. Catal. A: Gen. 177 (1999) 237.
[9] T. Okuhara, N. Mizuno, M. Misono, Adv. Catal. 41 (1996) 113.
[10] P.M. Price, J.H. Clark, K. Martin, D.J. Macquarrie, T.W. Bastock, Org. Process. Res. Dev. 2 (1998) 221.
[11] J.H. Clark, G.L. Monks, D.J. Nightingale, P.M. Price, J.F. White, J. Catal. 193 (2000) 348.
[12] (a) R.T. Sebulsky, A.M. Henke, Ind. Eng. Chem. Process Des. Dev. 10 (1971) 272;
(b) J.L.B. Tejero, A.M. Danvila, European Patent 0,353,813 (1990);
(c) G.D. Yadav, N.S. Doshi, Org. Process Res. Dev. 6 (2002) 263;
(d) B.M. Devassy, F. Lefebvre, W. Boehringer, J. Fletcher, S.B. Halligudi, J. Mol. Catal. A: Chem. 236 (2005) 162;
(e) G.D. Yadav, J.J. Nair, Micropor. Mesopor. Mater. 33 (1999) 1.
[13] C. De Castro, E. Sauvage, M.H. Volkenberg, W.F. Holderich, J. Catal. 196 (2000) 348.
[14] B.M. Devassy, F. Lefebvre, S.B. Halligudi, J. Catal. 231 (2005) 1.
[15] B.X. Luong, A.L. Petre, W.F. Hoelderich, A. Commarieu, J.-A. Laffitte, M. Espeillac, J.-C. Souchet, J. Catal. 226 (2004) 301.
[16] X. Hu, M.L. Foo, G.K. Chuah, S. Jaenicke, J. Catal. 195 (2000) 41.
[17] J.S. Beck, J.C. Vartuli, W.J. Roth, M.E. Leonowicz, C.T. Kresge, K.D. Schmitt, C.T.-W. Chu, D.H. Olson, E.W. Sheppard, S.B. McCullen, J.B. Higgins, J.L. Schlenker, J. Am. Chem. Soc. 114 (1992) 10834.
[18] E.R. Lachter, R.A. da S.S. Gil, D. Tabak, V.G. Costa, C.P.S. Chaves, J.A. dos Santos, React. Funct. Polym. 44 (2000) 1.
[19] A.B. Dixit, G.D. Yadav, React. Funct. Polym. 31 (1996) 237.
[20] J.F. Knifton, P.R. Anantaneni, P.E. Dai, M.E. Stockton, Catal. Lett. 75 (2001) 113.
[21] S. Sivasanker, A. Thangaraj, J. Catal. 138 (1993) 386.
[22] L.B. Young, US Patent, 4, 301, 317, 1981 to Mobil Oil Corporation.
[23] S. Sivasanker, A. Thangaraj, R.A. Abulla, P. Ratnasamy, Stud. Surf. Sci. Catal. 75 (1993) 397.
[24] (a) J.A. Kocal, B.P. Vora, T. Imai, Appl. Catal. A: Gen. 22 (2001) 295;
(b) S. Sivasanker, A. Thangaraj, R.A. Abulla, P. Ratnasamy, in: Proceedings of the International Congress on Catalysis, New Frontiers in Catalysis, vol. 75, Elsevier, Amsterdam, 1992, p. 397;
(c) A. Mourran, P. Magnoux, M. Guisnet, J. Chim. Phys. 92 (1995) 1394.
[25] Y. Cao, R. Kessas, C. Naccacha, Y.B. Taarit, Appl. Catal. A: Gen. 184 (1999) 231.
[26] J.A. Kocal, US Patent, 5, 196, 574, 1993 to UOP (Des Plaines, IL).
[27] J.F. Knifton, P.R. Anantaneni, P.E. Dai, US Patent, 5, 847, 254, 1998 to Huntsman Petrochemical Corporation (Austin, TX).
[28] P. Meriaudeau, Y.B. Taarit, A. Thangaraj, J.L.G. de Almeida, C. Naccache, Catal. Today 38 (1997) 243.
[29] T.-C. Tsai, I. Wang, S.-J. Li, J.-Y. Liu, Green Chem. 5 (2003) 404.
[30] C. Perego, P. Ingalliner, Catal. Today 73 (2002) 3.
[31] (a) P. Magnoux, A. Mourran, S. Bernard, M. Guisnet, Stud. Surf. Sci. Catal. 108 (1997) 107;
(b) P.B. Venuto, L.A. Hamilton, P.S. Landis, J.J. Wise, J. Catal. 4 (1966) 81;
(c) P.B. Venuto, L.A. Hamilton, P.S. Landis, J. Catal. 5 (1966) 484.
[32] K. Tanabe, W.F. Hoelderich, Appl. Catal. A: Gen. 181 (1999) 399.
[33] (a) M.L. Occelli (Ed.), Fluid Catalytic Cracking, American Chemical Society, Washington, DC, 1988;
(b) H.G. Karge, K. Hatada, Y. Zhang, R. Fiederow, Zeolites 3 (1983) 13;
(c) L.B. Zinner, K. Zinner, M. Ishige, A.S. Araujo, J. Alloys Compd. 193 (1993) 65;
(d) L.B. Zinner, A.S. Araujo, J. Alloys Compd. 180 (1992) 289;
(e) J.S. Magee, J.J. Balzek, in: J.A. Rabo (Ed.), Zeolite Chemistry and

Catalysis, American Chemical Society, Washington, DC, 2002, p. 615.
[34] (a) J. Biswas, I.E. Maxwell, Appl. Catal. 63 (1990) 197;
(b) M. Ikemoto, K. Tsutsumi, H. Takabashi, Bull. Chem. Soc. Jpn. 45 (1972) 1330.
[35] (a) N.N. Greenwood, A. Earnshaw, Chemistry of the Elements, second ed., Butterworth-Heinemann, Oxford, 1997;
(b) F.A. Cotton, G. Wilkinson, C.A. Murillo, M. Bochmann, Advanced Inorganic Chemistry, sixth ed., John Wiley and Sons Inc., New York, 1999.
[36] J.L.G. de Almeida, M. Dufaux, Y.B. Taarit, C. Naccache, Appl. Catal. A 114 (1994) 141–159.
[37] (a) B. Thomas, S. Sugunan, J. Porous Mater. 13 (2006) 99;
(b) B. Thomas, S. Prathapan, S. Sugunan, Micropor. Mesopor. Mater. 84 (2005) 137.
[38] S.G. Pataskar, PhD thesis University of Poona, Pune, 1984.
[39] A.V. Ramaswamy, Sci. Tech. Chim. Ind. (2000) 1.
[40] G. Engelhardt, in: G. Ertl, H. Knozinger, J. Weitkamp (Eds.), Handbook of Heterogeneous Catalysis, vol. 2, Wiley VCH, 1999, p. 536.
[41] G. Engelhardt, D. Michel, High Resolution Solid-State NMR of Silicates and Zeolites, Wiley, Chichester, 1987.
[42] (a) M. Weihe, M. Hunger, M. Breuninger, H.G. Karge, J. Weitkamp, J. Catal. 198 (2001) 299;
(b) M. Hunger, G. Engelhardt, J. Weitkamp, Micropor. Mater. 3 (1995) 497.
[43] (a) M.T. Melchior, D.E.W. Vaughan, A.J. Jacobson, J. Am. Chem. Soc. 104 (1982) 4859;
(b) M.T. Melchior, D.E.W. Vaughan, C.F. Pictroski, J. Phys. Chem. 99 (1995) 6128.
[44] J. Klinowski, T.A. Carpenter, L.F. Gladden, Zeolites 7 (1987) 73.
[45] E. Lippmma, M. Magi, A. Samoson, G. Engelhardt, A.H.R. Grimmer, J. Am. Chem. Soc. 102 (1980) 4889.
[46] Y.S. Chen, M. Guisnet, M. Kern, J.L.K. Lamberton, New J. Chem. 11 (1987) 623.
[47] E. O' Donoghue, D. Barthomeuf, Zeolites 6 (1986) 267.
[48] J.S. Beck, W.O. Haag, Alkylation of Aromatics, in: G. Ertl, H. Knozinger, J. Weitkamp (Eds.), Handbook of Heterogeneous Catalysis, vol. 5, Wiley, VCH, 1997, p. 2123.
[49] A.H. Peterson, B.L. Phillips, J.T. Kelly, Ind. Eng. Chem. 4 (1965) 261.
[50] H.R. Alul, Ind. Eng. Chem. Prod. Res. Dev. 7 (1968) 7.
[51] C.D. Nenitzescue, Rev. Roumaine Chim. 9 (1964) 5.
[52] B. Wang, W. Lee, T.X. Cai, S.-E. Park, Catal. Lett. 76 (2001) 1.
[53] (a) Z. Da, H. Han, P. Magnoux, M. Guisnet, Appl. Catal. A: Gen. 219 (2001) 45;
(b) M. Guisnet, P. Magnoux, Appl. Catal. 54 (1989) 1;
(c) Z. Da, P. Magnoux, M. Guisnet, Appl. Catal. A: Gen. 182 (1999) 407;
(d) S. Sivasanker, in: B. Viswanathan, S. Sivasanker, A.V. Ramaswamy (Eds.), Catalysis Principles and Applications, Narosa Publishing House, New Delhi, 2002, p. 253.